Impaired V(D)J Recombination and Lymphocyte Development in Core RAG1–expressing Mice

Darryll D. Dudley,[1] JoAnn Sekiguchi,[1] Chengming Zhu,[1] Moshe J. Sadofsky,[2] Scott Whitlow,[1] Jeffrey DeVido,[1] Robert J. Monroe,[1] Craig H. Bassing,[1] and Frederick W. Alt[1]

[1]*Howard Hughes Medical Institute, The Children's Hospital, The Center for Blood Research, Harvard Medical School, Boston, MA 02115*
[2]*Department of Pathology, Albert Einstein College of Medicine, Bronx, NY 10461*

Abstract

RAG1 and RAG2 are the lymphocyte-specific components of the V(D)J recombinase. In vitro analyses of RAG function have relied on soluble, highly truncated "core" RAG proteins. To identify potential functions for noncore regions and assess functionality of core RAG1 in vivo, we generated core RAG1 knockin (RAG1$^{c/c}$) mice. Significant B and T cell numbers are generated in RAG1$^{c/c}$ mice, showing that core RAG1, despite missing ∼40% of the RAG1 sequence, retains significant in vivo function. However, lymphocyte development and the overall level of V(D)J recombination are impaired at the progenitor stage in RAG1$^{c/c}$ mice. Correspondingly, there are reduced numbers of peripheral RAG1$^{c/c}$ B and T lymphocytes. Whereas normal B lymphocytes undergo rearrangement of both J_H loci, substantial levels of germline J_H loci persist in mature B cells of RAG1$^{c/c}$ mice, demonstrating that DJ_H rearrangement on both IgH alleles is not required for developmental progression to the stage of V_H to DJ_H recombination. Whereas V_H to DJ_H rearrangements occur, albeit at reduced levels, on the nonselected alleles of RAG1$^{c/c}$ B cells that have undergone D to J_H rearrangements, we do not detect V_H to D_H rearrangements in RAG1$^{c/c}$ B cells that retain germline J_H alleles. We discuss the potential implications of these findings for noncore RAG1 functions and for the ordered assembly of V_H, D_H, and J_H segments.

Key words: antigen receptor • DNA cleavage • RS • hybrid joint • immune deficiency

Introduction

Ig and TCR variable region genes are assembled during early lymphocyte development from component variable (V), diversity (D), and joining (J) gene segments. V(D)J recombination is initiated by the RAG1 and RAG2 proteins via introduction of DNA double strand break (DSBs) between the V, D, and J coding segments and flanking recombination signal (RS) sequences. RAG1 and RAG2 are necessary in vivo and sufficient in vitro for initiation of V(D)J recombination (for review see reference 1). After DNA cleavage, RAG-cleaved coding and RS ends are joined by ubiquitously expressed, nonhomologous end-joining (NHEJ) proteins (for review see reference 2).

V(D)J recombination is tightly regulated during lymphocyte development within the context of lymphocyte lineage specificity, developmental stage specificity, and feedback regulation of allelic exclusion (for reviews see references 2, 3). Furthermore, the developmental progression of lymphocytes requires the productive assembly and expression of antigen receptor genes. In developing B lymphocytes, IgH genes are assembled before IgL genes; whereas in developing αβ T cells, TCRβ genes are assembled before TCRα genes (for review see reference 3). Both IgH and TCRβ genes are assembled via an ordered process in which D to J rearrangements proceed to completion on both alleles, followed by V segment rearrangement to a preexisting DJ complex (4, 5). Productive rearrangement and expression of IgH μ chains in ckit$^+$/B220^{int}/CD43$^+$/CD25$^-$/CD19$^+$ progenitor (pro–)B cells and TCRβ chains in CD4$^-$CD8$^-$

(double negative [DN]) pro–T cells induces cellular expansion and differentiation, respectively, to the corresponding ckit⁻/B220⁺/CD43^{lo}/CD25⁻/CD19⁺ pre–B cell stage and the CD4⁺/CD8⁺ (double positive [DP]) thymocyte stage (6, 7). Functional rearrangement and expression of IgL or TCRα chains as part of surface IgM or αβ TCR signals precursor B or T lymphocytes to develop into mature peripheral lymphocytes (for reviews see references 7, 8).

Biochemical activities of the RAG1 and RAG2 proteins have been extensively characterized in vitro using purified proteins and defined DNA substrates (for review see reference 9). Full-length RAG proteins are largely insoluble when overproduced; consequently, in vitro studies have used truncated "core" RAG proteins. Core RAG1 (aa 384–1,008 of 1,040 residues) and core RAG2 (aa 1–383 of 527 residues) comprise the minimal regions of RAG1 and RAG2 necessary for recombination of extrachromosomal substrates in nonlymphoid cells (10–13). Whereas core RAGs mediate the basic V(D)J recombination reaction in vitro, the activities of these truncated proteins are not identical to those of full-length RAGs. In this context, noncore RAG regions influence both V(D)J recombination efficiency and products formed when assayed in cell lines (14–19).

Noncore RAG regions are evolutionarily conserved, suggesting these regions may serve important functions (11). Studies of A-MuLV–transformed pre–B cells have implicated noncore RAG regions in accessory and/or regulatory functions in chromosomal V(D)J recombination (18, 19). Thus, NH₂-terminal elements of RAG1 are required for complete D$_H$ to J$_H$ rearrangement in A-MuLV transformants (19), whereas the COOH terminus of RAG2 may be more important for V$_H$ to DJ$_H$ rearrangement than for D$_H$ to J$_H$ rearrangement (18). In this regard, mice expressing core RAG2 in place of endogenous RAG2 (which we will refer to here as RAG2$^{c/c}$) display impaired lymphocyte development at the pro–B and pro–T cell stages, accompanied by decreased levels of V to DJ rearrangement (20, 21). Inactivating mutations in *RAG1* or *RAG2* lead to a complete block in lymphocyte development in mice (22, 23) and are a cause of human T⁻B⁻ SCID (24, 25). However, missense mutations in *RAG1* or *RAG2* that result in reduced, and possibly altered, V(D)J recombinase activity lead to Omenn Syndrome (OS), a disease characterized by lack of B cells and a reduced, oligoclonal T cell repertoire (24, 26). In addition, frameshift mutations in noncore *RAG1* regions can result in NH₂-terminal RAG1 truncations that lead to OS–like immunodeficiencies (27, 28). To address the role of noncore RAG1 regions in vivo, we have generated mice containing specific replacement of the full-length endogenous *RAG1* gene with a gene encoding the mouse core RAG1 protein.

Materials and Methods

Antibodies and Flow Cytometry. Single cell suspensions from lymphoid tissues were stained with antibodies conjugated to FITC, PE, and cytochrome C (CyC) by standard procedures. The following antibody conjugates (BD Biosciences and Southern Biotechnology Associates, Inc.) were used: CyC anti-CD44, PE anti-CD25, CyC anti-CD4, FITC anti-CD8, FITC anti-CD43, FITC anti-GR1, FITC anti-TCRγ,δ, CyC and FITC anti-B220, and PE anti-IgM. A total of eight RAG$^{c/c}$ mice, six RAG$^{+/c}$, and six RAG$^{+/+}$ mice between three and five wk of age were analyzed. pro– and pre–B cell populations were sorted based on CD43 and B220 expression after gating out all cells staining with IgM. Cell sorting was performed on independent BM samples from five RAG1$^{c/c}$, one RAG1$^{+/c}$, and four RAG1$^{+/+}$ littermates.

Generation and Analysis of B Cell Hybridomas. Single cell splenocyte suspensions from RAG1$^{+/+}$, RAG1$^{+/c}$, and RAG1$^{c/c}$ mice were cultured with anti-CD40 (1 μg/ml) and IL-4 (10 ng/ml) for 4 d and activated B cells fused to the NS-1 fusion partner (ATCC TIB-18). Hybridomas were screened for isotype secretion by sandwich ELISA using isotype-specific antibodies from SBA. Genomic DNA from each Ig-secreting hybridoma was assayed for Ig rearrangements by Southern blotting. J$_H$ rearrangement status and the number of alleles was determined via a J$_H$–specific probe on StuI- or EcoRI-digested DNA (29). V$_H$ to DJ$_H$ rearrangements were detected with a probe from 5′ of DFL16; V$_H$ to DJ$_H$ rearrangements will result in deletion of this fragment (hybridomas nos. 10 and 12); whereas nonrearranged alleles or D to J$_H$ rearranged alleles will retain this band. DFL16 to J$_H$ joins will result in a band of unique size. Nonrearranged J$_H$ alleles were confirmed by Southern blot analyses using a probe from 3′ of DQ52 (30). D to J$_H$ rearrangements result in deletion of this fragment; thus, alleles that have not undergone D$_H$ to J$_H$ rearrangements will retain this germline band. Cell lines with only one detectable IgH allele originating from B cells were not further analyzed.

Purification of B and T Cell Fractions. Single cell suspensions of splenocytes from RAG1$^{+/+}$, RAG1$^{+/c}$, and RAG1$^{c/c}$ were cultured with anti-CD40 and IL4 for B cell activation or ConA and IL-2 for T cell activation. Activated B cells from day 2 cultures were purified using biotinylated anti-CD19–specific antibodies in conjunction with streptavidin-conjugated MACS microbeads and MACS Separation Columns (Miltenyi Biotech). T cells cultured with ConA + IL-2 for 6 d were purified by Lympholyte-M sedimentation (Cedarlane). Purity of separated B and T cells was analyzed by flow cytometry and found to be at least 90%. DP T cell DNA was isolated by staining thymocytes with FITC anti-CD4 and PE anti-CD8 antibodies and sorting on a MO-Flo (Becton Dickinson). DN3 thymocyte DNA was isolated by first depleting CD4⁺ thymocytes using anti-CD4-conjugated MACS microbeads and staining the unbound cell fraction with CYC anti-CD44, PE anti-CD25, and a combination of FITC anti-CD4, -CD8, -B220, -Mac1, -GR1, and -TCRγ,δ antibodies and sorting on live-gated FITC⁻, CYC⁻, and PE⁺ cells.

PCR Analysis of IgH and TCR Rearrangements. Genomic DNA from sorted pro– and pre–B cell populations and purified CD4⁺CD8⁺ DP or CD4⁻CD8⁻CD44⁻CD25⁺ DN3 T cells was analyzed for IgH and TCRβ rearrangements by PCR amplification (31, 32). LMPCR for SE breaks were performed as described previously (33). Oligos and PCR primers are listed in Table S1 (available at http://www.jem.org/cgi/content/full/jem.20030627/DC1). Briefly, PCR reactions contained 90, 30, 10, and 3.3 ng or 250, 50, 10 and 2 ng of genomic DNA for IgH and TCRβ amplifications, respectively, 20 pmol of each primer, 0.2 mM dNTPs, 50 mM KCl, 10 mM Tris-HCl (pH 8.0), 2.5 mM MgCl₂, and 0.5 U QIAGEN Taq polymerase. Amplification conditions were as follows: 94°C for 45 s, 60°C for 1 min, 72°C for 2.5 min for 30 cycles. Amount of input genomic DNA was normalized by PCR amplification of a coding exon of the ATM

gene. PCR products were analyzed by agarose gel electrophoresis, transferred to Zetaprobe membrane, and probed with nested oligonucleotide probes to detect rearrangements. PCR analyses were performed at least three times on genomic DNA samples from sorted B cells and purified T cells, respectively, isolated from at least three RAG1[c/c] mice and either RAG1[+/c] or RAG1^{+/+} littermates.

Generation of Core RAG1 Mice. The pMS127 plasmid containing the core RAG1 coding sequence and three copies of a human c-Myc tag at the COOH-terminal end was provided by M. Sadofsky (Albert Einstein College of Medicine) (11). The core RAG1 coding sequence contains a single nucleotide change (A to G) that results in a methionine to valine substitution at position 484. A similar form, with an additional 9-residue Histidine COOH-terminal tag, has been used extensively in vitro to define the biochemical and V(D)J recombination activities intrinsic to the RAG recombinase (34–36) 2.1 kb of homologous sequence immediately 5′ of RAG1 was cloned along with core RAG1 coding sequence into the SalI site of pLNTK (37). A 3.3-kb MluI to BamH1 fragment was cloned into the XhoI site to complete

the core RAG1 replacement vector. TC1 embryonic stem cells (provided by P. Leder, Harvard Medical School) were transfected with the targeting vector as described previously (38). A positively selected recombinant was identified by Southern blotting using the 5′ and 3′ targeting probes (Fig. S1, available at http://www.jem.org/cgi/content/full/jem.20030627/DC1). The LoxP flanked neomycin resistance (Neo[r]) gene was deleted by transiently transfecting the ES cell clone with a plasmid-based Cre recombinase expression construct (37). Subclones of this ES cell line were injected into C57Bl/6 blastocysts to generate chimeric mice. RAG1[+/c] mice were intercrossed to produce 129sv RAG1[c/c] mice.

Results

The Generation of Mice that Express the Core RAG1 Protein. To evaluate in vivo functions of noncore RAG1 regions, we used gene targeting to replace the endogenous *RAG1* gene with a recombinant gene encoding the mouse
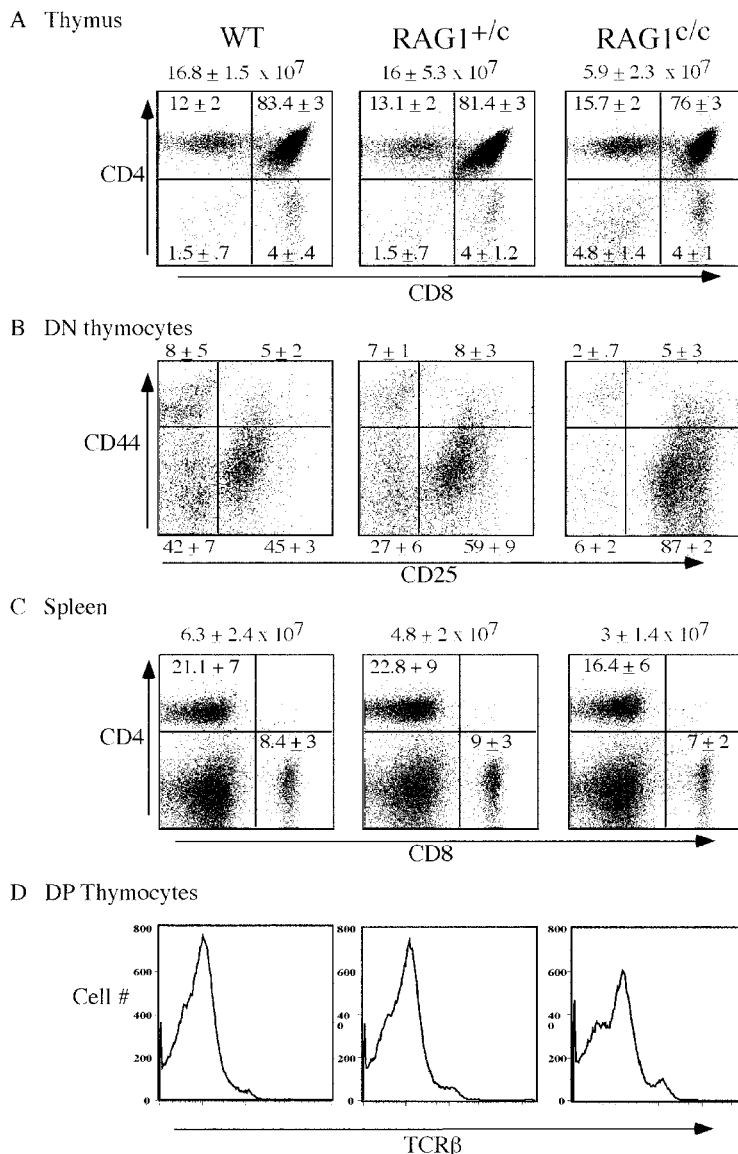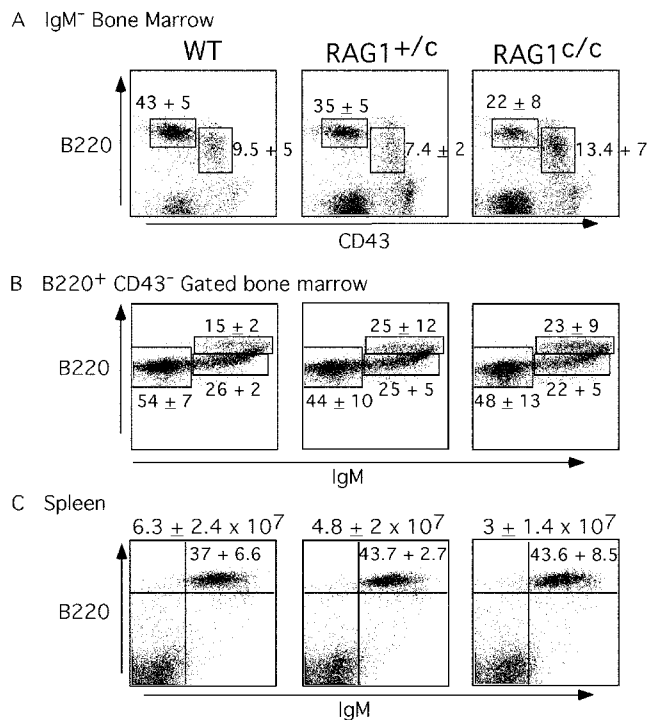

Figure 1. Flow cytometric analysis of T cell development in RAG1[c/c] mice. (A) FACS® analysis was performed on thymocytes isolated from RAG1[c/c], RAG1[+/c], and RAG1^{+/+} littermates stained with CyC anti-CD4 and PE anti-CD8. (B) Double negative thymocytes stained with PE anti-CD44 and FITC anti-CD25 after electronically gating out CD4, CD8, TCR-γ,δ, B220, and GR-1 positively staining cells. (C) Splenocytes from RAG1[c/c], RAG1[+/c], and RAG1^{+/+} littermates were stained with CyC anti-CD4 and PE anti-CD8 antibodies. (D) Thymocytes were stained with FITC anti-TCRβ after electronically gating on CD4+CD8+ DP cells. Mice were analyzed at 3–5 wk of age; representative data are shown. Total thymus cell counts are indicated over the panels in A, and total spleen cell counts are indicated over the panels in C.

core RAG1 protein (aa 384–1008) (Fig. S1, available at http://www.jem.org/cgi/content/full/jem.20030627/DC1). We first generated targeted ES clones with endogenous *RAG1* replaced on a single allele by the synthetic core *RAG1* gene and a 3′*loxP*-PGK–Neo^r cassette (Fig. S1, A and B). We then used transient expression of Cre recombinase to delete the PGK–Neo^r cassette (Fig. S1 B). Chimeric mice from Cre-deleted ES cell clones were bred to 129sv mice to obtain mice carrying the core *RAG1* gene in their germline. Heterozygous core *RAG1* (RAG1$^{+/c}$) mice were intercrossed to produce RAG1$^{c/c}$ mice and RAG1$^{+/c}$ and RAG1$^{+/+}$ littermate controls (Fig. S1 C). The core RAG1 protein was expressed at elevated levels compared with the full-length protein, as predicted by previous studies (13, 15), and was found mostly in nuclear extracts (Fig. S1 D). RAG1$^{c/c}$ mice were housed in a pathogen-free environment and survived into adulthood without overt defects.

Core RAG1 Mice Exhibit Impaired Lymphocyte Development. We found reduced thymic cellularity of RAG1$^{c/c}$ mice compared with RAG1$^{+/c}$ and RAG1$^{+/+}$ control mice (average thymocyte count for RAG1$^{c/c}$ thymuses = 29% ± 11% of controls; Fig. 1 A). FACS$^®$ analyses of RAG1$^{c/c}$ thymocytes demonstrated an almost normal distribution of CD4$^+$/CD8$^+$ (DP) and CD4$^+$/CD8$^-$ or CD4$^-$/CD8$^+$ (single positive) populations (Fig. 1 A). However, RAG1$^{c/c}$ mice accumulated CD4$^-$/CD8$^-$ (DN) pro–T cells with a strikingly high percentage of cells amassing at the CD25$^+$CD44$^-$ (DN3) stage compared with RAG1$^{+/c}$ and RAG1$^{+/+}$ control mice (Fig. 1 B). TCRβ rearrangements are completed within the DN3 stage, with productive TCRβ expression inducing cellular proliferation, differentiation to the CD25$^-$CD44$^-$ DN4 stage, and cessation of further Vβ to DJβ rearrangement (allelic exclusion) (for review see reference 39). Thus, the accumulation of RAG1$^{c/c}$ DN3 thymocytes is consistent with diminished capacity of core RAG1 to efficiently mediate complete VβDJβ rearrangements.

TCRα chain expression is not required for the DN to DP transition (for reviews see references 7, 39). However, we found an increased ratio of TCRβ^{lo} to TCRβ^{int} DP thymocytes in RAG1$^{c/c}$ mice compared with controls (Fig. 1 D). This is consistent with delayed TCRα rearrangement, since DP thymocytes from mice that lack either the TCRα enhancer or TCRα genes likewise express low levels of TCRβ at their cell surface in the absence of TCRα chains (40, 41). We did not detect TCRβ$^-$ DP thymocytes in RAG1$^{c/c}$ mice, confirming that delayed development due to decreased V(D)J recombination efficiency does not allow progression to the DP stage in the absence of TCRβ gene expression (Fig. 1 D). The absolute numbers of splenic αβ T cells in RAG1$^{c/c}$ mice were reduced ~50% from that of RAG1$^{+/c}$ and RAG1$^{+/+}$ controls (Fig. 1 C). We conclude that overall T cell development in RAG1$^{c/c}$ mice is impaired with respect to the pro– to pre–T cell transition, accompanied by a modest reduction in overall T cell numbers.

We detected a statistically significant reduction in the percentage and absolute number of CD43^{lo}B220$^+$ pre–B

Figure 2. Flow cytometric analysis of B cell development in RAG1$^{c/c}$ mice. (A) FACS$^®$ analysis was performed on RBC-free BM cells isolated from both femurs of individual RAG1$^{c/c}$, RAG1$^{+/c}$, and RAG1$^{+/+}$ littermates stained with CyC anti-B220, FITC anti-CD43, and PE anti-IgM antibodies and gated on the IgM$^-$ population. B220^{int}CD43$^+$ pro–B and B220$^+$CD43^{lo} pre–B cell populations are shown. (B) B220$^+$CD43^{lo} BM cells were further stained with PE anti-IgM to determine the percentage of BM cells in Hardy fractions D, E, and F. (C) Splenocytes from RAG1$^{c/c}$, RAG1$^{+/c}$, and RAG1$^{+/+}$ littermates were stained with CyC anti-B220 and PE anti-IgM antibodies. Mice were analyzed at 3–5 wk of age; representative data are shown. Total spleen cell counts are indicated over the bottom panels.

cells in RAG1$^{c/c}$ mice relative to RAG1$^{+/c}$ and RAG1$^{+/+}$ control mice (average pre–B cell count RAG1$^{c/c}$ BM = 6.5 ± 2.9 × 10^5 versus 10.3 ± 1.3 × 10^5 in control littermates, P = .020 by paired *t* test; Fig. 2 A) (6). Correspondingly, the absolute splenic B cell numbers in RAG1$^{c/c}$ mice were ~50% of those in control mice (Fig. 2 C). On the other hand, absolute BM CD43$^+$B220^{int} pro–B cell numbers were relatively normal in RAG1$^{c/c}$ mice (average pro–B cell count RAG1$^{c/c}$ BM = 5.2 ± 1.7 × 10^5 versus 5.5 ± 1.5 × 10^5 in control littermates); and the percentages of Hardy fractions D, E, and F in the BM of RAG1$^{c/c}$ and littermate controls were also comparable (Fig. 2, A and B) (6). Therefore, B cell development in RAG1$^{c/c}$ mice shows a modest impairment in the pro– to pre–B cell transition and a corresponding reduction in overall B cell numbers.

TCRβ and TCRα Gene Rearrangements in RAG1$^{c/c}$ Mice. Since RAG1$^{c/c}$ mice exhibit impaired T cell development, we assayed for potential alterations in TCRβ rearrangement. We employed PCR primers located 5′ of Dβ1 or Dβ2 and 3′ of Jβ1 or Jβ2 to amplify Dβ1 to Jβ1 and Dβ2 to Jβ2 rearrangements from purified CD44$^-$CD25$^+$ DNIII or DP thymocytes from RAG1$^{c/c}$ and control mice
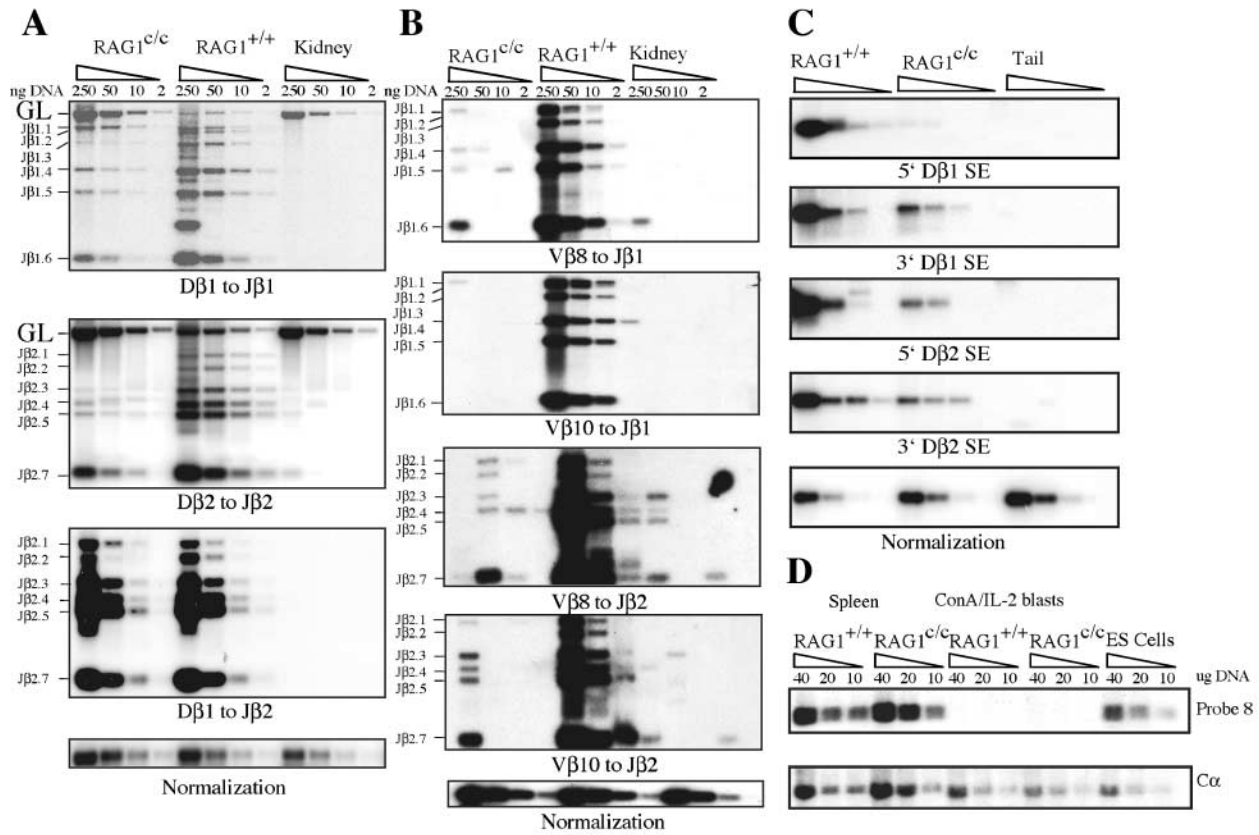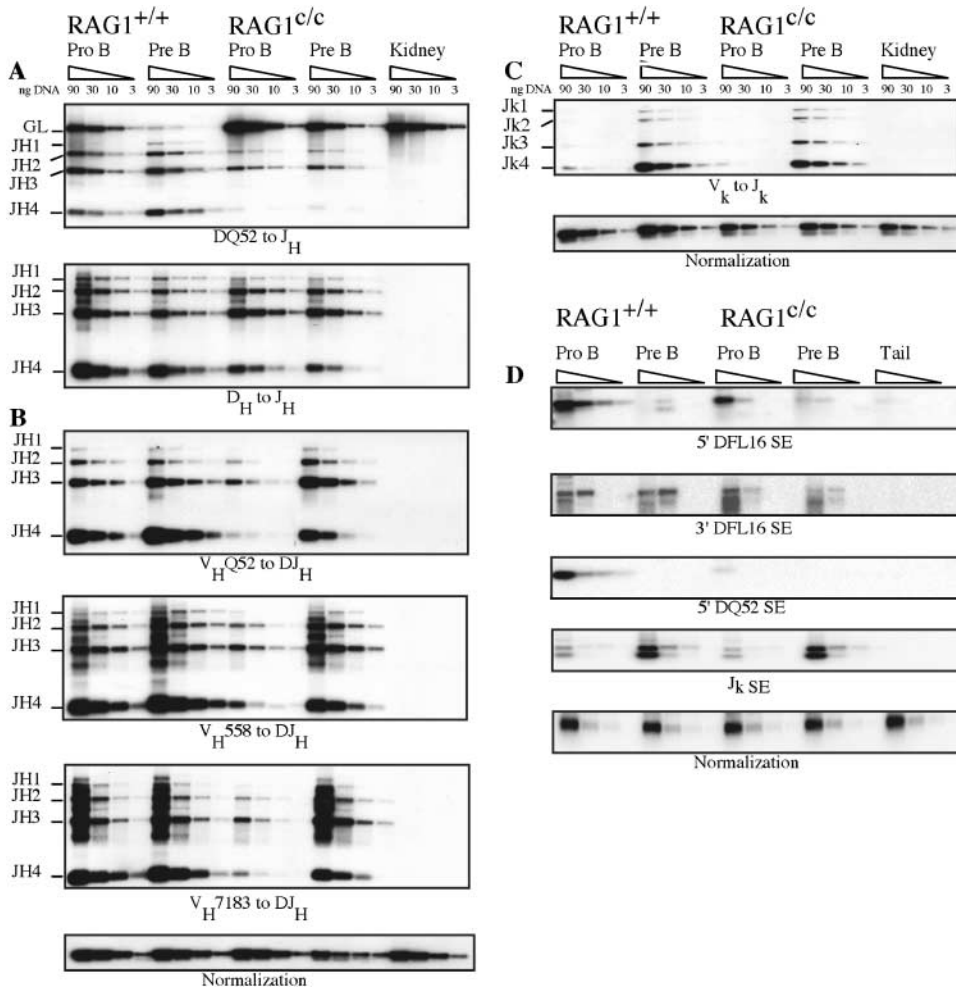
Figure 3. TCRβ rearrangements. Genomic DNA from sorted CD44⁻CD25⁺ DN3 T cells or nonrearranged control tissue (kidney) from RAG1$^{+/+}$ and RAG1$^{c/c}$ mice was isolated and subjected to PCR amplification of D to Jβ1 and D to Jβ2 (A) and V to DJβ1 and V to DJβ2 (B) rearrangements. PCR amplification was performed on serial fivefold dilutions of genomic DNA, and the products were detected by Southern blot hybridization. Control PCR amplification of a nonrearranging locus was also performed to normalize levels of input DNA. (C). LMPCR was used to detect RS broken signal ends from 5′ Dβ1, 3′ Dβ1, 5′ Dβ2, and 3′ Dβ2 in DNA of sorted DN3 thymocytes isolated from RAG1$^{c/c}$ and RAG1$^{+/+}$ mice as described previously (21, 63). Fivefold serially diluted linker ligated DNA is shown along with a PCR reaction of a nonrearranging locus as a loading control. (D). Southern blot analysis on Eco0109-digested DNA isolated from spleen of purified day 6 ConA + IL-2 activated splenic T cells to determine the extent of TCRα rearrangement as described previously (40).

(32). The levels of PCR products representing most Dβ1 to Jβ1 rearrangements were reduced in DNA isolated from DN3 T cells of RAG1$^{c/c}$ mice compared with controls (Fig. 3 A). Similarly, Dβ2 to Jβ2 levels were reduced and were accompanied by increased levels of germline Dβ2/Jβ2 bands (Fig. 3 A). In contrast, Dβ1 to Jβ2 rearrangement levels were comparable between RAG1$^{c/c}$ and control mice (Fig. 3 A). We found a similar reduction in Dβ1 to Jβ1 and Dβ2 to Jβ2 rearrangements in DNA isolated from sorted RAG1$^{c/c}$ DP thymocytes, but Dβ1 to Jβ2 rearrangements again were not markedly changed (Fig. S2 A, available at http://www.jem.org/cgi/content/full/jem.20030627/DC1). There was also a diminished level of 3′ Dβ broken RS ends in DN3 thymocyte DNA from RAG1$^{c/c}$ mice, consistent with reduced RS cleavage by core RAG1 (Fig. 3 C).

We employed Vβ8– and Vβ10-specific primers in conjunction with 3′ Jβ1 or 3′ Jβ2 primers to determine whether Vβ rearrangement is altered in RAG1$^{c/c}$ versus WT mice. Vβ8 and Vβ10 rearrangements to either Jβ1 or Jβ2 were dramatically reduced in RAG1$^{c/c}$ DN3 thy-

mocytes (Fig. 3 B). Likewise, 5′Dβ RS ends were also reduced in RAG1$^{c/c}$ DN3 thymocytes, consistent with reduced RAG-mediated cleavage during Vβ to DJβ rearrangement (Fig. 3 C). Conversely, there was little or no reduction in Vβ8 or Vβ10 to Jβ2 rearrangements in RAG1$^{c/c}$ DP thymoyctes (Fig. S2, A and B), as expected given selection for at least one (productive) Vβ(D)Jβ rearrangement in each DP cell. Therefore, the ability of core RAG1 to mediate TCRβ rearrangements in vivo appears compromised for both the Dβ to Jβ and Vβ to DJβ steps. In WT mice, TCRα genes rearrange on both alleles during the DP T cell stage; thus, all mature T cells will have deleted the sequences located between the 3′ most Vα and 5′ most Jα segments (42). Southern blot analysis using a probe from between Vα and Jα gene segments (probe 8) (40) demonstrated that both TCRα alleles rearrange to completion in mature T cells of RAG1$^{c/c}$ and WT mice (Fig. 3 D). Although this finding does not rule out a modest reduction in TCRα rearrangement in RAG1$^{c/c}$ DP cells, it shows that overall TCRα gene rearrangements are not substantially altered.

Figure 4. IgH rearrangements. Genomic DNA from sorted pro– and pre–B cell populations from RAG1$^{+/+}$ and RAG1$^{c/c}$ littermates was isolated and subjected to PCR amplification of D to J$_H$ (A), V to DJ$_H$ (B), and V$_\kappa$ to J$_\kappa$(C) rearrangements. PCR amplification was performed on serial threefold dilutions of genomic DNA, and the products were detected by Southern blot hybridization. Control PCR amplification of a nonrearranging locus was also performed to normalize levels of input DNA. One of four experiments performed on independent sets of sorted B cell samples is shown. (D). LMPCR was used to detect RS broken signal ends from the indicated RSSs in DNA of sorted pro– and pre–B cells isolated from RAG1$^{c/c}$ and RAG1$^{+/+}$ mice as described previously (21, 63). Fivefold serially diluted linker ligated DNA is shown along with a PCR reaction of a nonrearranging locus as a loading control.

Rearrangements of IgH and Igκ in RAG1$^{c/c}$ Mice. We used a PCR approach to analyze D$_H$ to J$_H$ and V$_H$ to DJ$_H$ rearrangements in sorted CD43$^+$B220^{int} pro–B and CD43^{lo}B220$^+$ pre–B cells of RAG1$^{c/c}$ and control mice. Normal B cells usually rearrange D$_H$ to J$_H$ on both IgH alleles (4, 6). Moreover, all pre–B cells, based on selection for IgH μ chain expression, will have a productive V$_H$DJ$_H$ rearrangement on one of their two J$_H$ alleles (43). Approximately 40% of normal mature B cells have a nonproductive V$_H$DJ$_H$ rearrangement on their second nonselected allele, with the remaining ~60% having a DJ$_H$ rearrangement on the second nonselected allele (4). Therefore, the overall level of V$_H$ to DJ$_H$ rearrangements can be reduced by, at most, ~30% in pre–B or mature B cell populations. Consequently, PCR methods cannot accurately quantify the effects on V$_H$ to DJ$_H$ rearrangement in these populations. However, PCR can be used to assay for overall reduction in the level of D$_H$ to J$_H$ recombination, which would be reflected by increased levels of germline alleles.

We employed PCR primers located 5′ of D$_H$Q52 and 3′ of the J$_H$4 gene segment to amplify D$_H$Q52 to J$_H$ rearrangements. Assembled D$_H$Q52J$_H$ complexes can be excised from the chromosome upon subsequent rearrangement of 5′ D$_H$ segments with 3′ J$_H$ gene segments (44, 45).

Therefore, the use of a 3′ primer downstream of J$_H$4 permits specific amplification of D$_H$Q52 to J$_H$ rearrangements retained within the IgH locus on alleles that lack V$_H$ to DJ$_H$ rearrangements. Joining of D$_H$Q52 to J$_H$ segments, especially J$_H$4, was reduced in both RAG1$^{c/c}$ pro–B and pre–B cells (Fig. 4 A). Consistent with reduced DJ$_H$ joining, we observed increased levels of germline J$_H$ alleles, most notably in the pre–B cell population (Fig. 4 A). We conclude that RAG1$^{c/c}$ pro–B and pre–B cells have reduced levels of D$_H$Q52 to J$_H$ rearrangements. To examine other D$_H$ segments, we employed a degenerate 5′ D$_H$ RS primer (31) to amplify most D$_H$ to J$_H$ rearrangements. The level of D$_H$ to J$_H$1 and J$_H$4 rearrangements also was reduced in both RAG1$^{c/c}$ pro– and pre–B cells, but D$_H$ rearrangements to J$_H$2 and J$_H$3 were present at control levels (Fig. 4 A). Notably, the level of 3′ DFL16 RS ends did not appear to be markedly reduced in RAG1$^{c/c}$ pro–B cells (Fig. 4 D).

We also analyzed rearrangement of three frequently used V$_H$ gene segment families (V$_H$7183, V$_H$Q52, and V$_H$558) in RAG1$^{c/c}$ B lineage cells. We employed a 3′ J$_H$4 primer along with 5′ primers specific to these V$_H$ families to amplify family-specific V$_H$DJ$_H$ rearrangements (31). Rearrangement of all three V$_H$ families were reduced in RAG1$^{c/c}$ pro–B cells (Fig. 4 B). However, in RAG1$^{c/c}$ pre–B cells,

rearrangements of these same V_H families were only modestly reduced (Fig. 4 B). As outlined above, this is not surprising because all pre–B cells will have at least one productive V_HDJ_H rearrangement. Overall utilization of tested V_H families in pro– or pre–B cells was not dramatically altered (Fig. 4 B), indicating that, at least at a gross level, usage of endogenous V_H families by core RAG1 is not obviously influenced by RS sequence [RSS] or V_H chromosomal location. We also detected a reduction in the level of 5′DFL16 and 5′DQ52 RS ends in the DNA of pro–B cells, indicating a reduced capacity of core RAG1 to mediate V_H to DJ_H RS cleavage compared with full-length RAG1 (Fig. 4 D). Therefore, RAG1$^{c/c}$ pro–B cells have reduced overall levels of V_HDJ_H rearrangements but relative utilization of different V_H families is not markedly altered.

To analyze Igκ rearrangements, we performed PCR analyses on DNA isolated from sorted pro– and pre–B cells using a $V_κ$-specific primer in conjunction with a primer located downstream of $J_κ4$. We detected equivalent levels of $V_κ$ to $J_κ$ rearrangements in pre–B cells of RAG1$^{c/c}$ and control mice, indicating that the noncore regions of RAG1 are not required for accumulation of normal levels of $V_κ$ to $J_κ$ rearrangements (Fig. 4 C). We also found an equivalent level of 5′ $J_κ1$ RS ends in pre–B cells of RAG1$^{c/c}$ and control mice, consistent with the finding that $V_κ$ to $J_κ$ rearrangements are not substantially diminished (Fig. 4 D).

Mature B Cells with Germline J_H Alleles in RAG1$^{c/c}$ Mice. Normally, D_H to J_H rearrangement occurs on both IgH alleles in developing pro–B cells before the onset of V_H to

DJ_H rearrangement (6). However, our PCR analyses suggested possible retention of germline J_H alleles in RAG1$^{c/c}$ pre–B cells. To confirm this, we performed Southern blot analyses on genomic DNA from purified CD19$^+$ splenic B cells of RAG1$^{c/c}$ and control mice using a J_H-specific probe. Whereas RAG1$^{+/+}$ B cells had, as expected, little or no unrearranged J_H loci, RAG1$^{c/c}$ B cells contained a substantial level of the germline-sized J_H fragment (Fig. 5 and not depicted). To more precisely quantify the reduction in J_H rearrangements on the nonproductive allele in RAG1$^{c/c}$ B cells, we analyzed J_H rearrangements in B cell hybridomas. Previous analyses have shown that a low percentage of hybridomas from WT mice retain germline J_H alleles (4, 30), despite the fact that essentially no germline J_H locus is detectable in purified splenic B cells (4, 46). These findings suggested that WT hybridomas with germline J_H alleles most likely result from tripartite fusions involving non–B lineage cells. Consistent with prior studies (30), Southern blot analyses revealed that most control hybridomas had rearrangements of both J_H alleles; although a few retained a germline-sized band (Table I). In dramatic contrast, 59% of the RAG1$^{c/c}$ B cell hybridomas contained a germline J_H allele (Fig. 5, A and C; Table I). This very high level of retained germline J_H alleles in RAG1$^{c/c}$ B cell hybridomas confirms the findings with purified CD19$^+$ B cells (Fig. 5 and not depicted). Therefore, expression of core RAG1 in the absence of WT RAG1 results in a developmentally altered pattern of IgH locus rearrangement in which V_H to DJ_H rearrangements frequently occur in developing
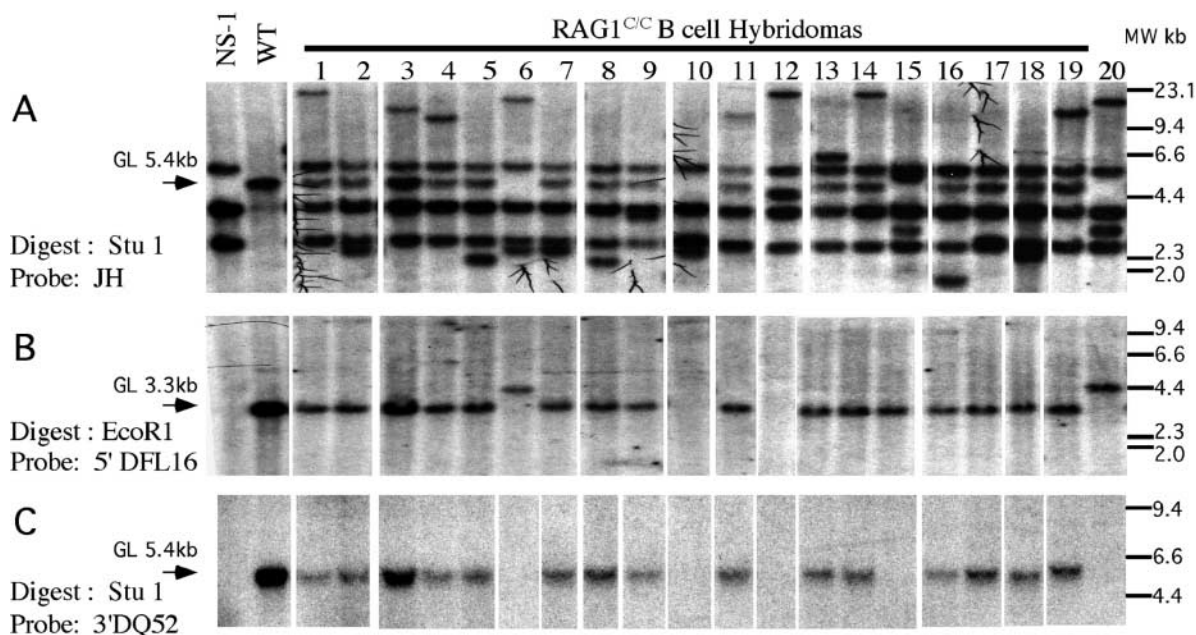
Figure 5. IgH rearrangement status in RAG1$^{c/c}$ B cell hybridomas. Genomic DNA was isolated from RAG1$^{c/c}$ hybridoma cell lines shown to secrete Ig, and the rearrangements were examined by Southern blot analysis. (A). Southern blot analysis of hybridoma DNA using a J_H-specific probe on StuI-digested DNA for determining J_H rearrangement status. (B). Southern blot analysis of hybridoma DNA using a 5′ DFL16-specific probe on EcoR1-digested DNA for determining V_H to DJ_H rearrangement status. (C). Southern blot analysis of hybridoma DNA using a 3′ DQ52-specific probe on Stu1-digested DNA for confirming germline IgH rearrangement status. Arrows indicate two hybridomas with V_HDJ_H rearrangements on both IgH alleles. The presence of two IgH alleles was confirmed by Southern blot hybridization with the J_H probe on EcoR1-digested DNA. Representative data are shown.

Table I. *IgH Status of Hybridomas Derived from Rag1$^{+/+}$ or Rag1$^{c/c}$ B Cells*

Genotype	Experiment	V(D)J/DJ	V(D)J/V(D)J	V(D)J/germline	Total
		(%)	*(%)*	*(%)*	
RAG$^{+/+}$	Fusion 1	14 (61)	7 (30)	2 (9)	23
	Fusion 2	7 (64)	3 (27)	1 (9)	11
	Fusion 3	5 (63)	2 (25)	1 (12)	8
	Total	26 (63 ± 2)	12 (27 ± 3)	4 (10 ± 2)	42
RAG1$^{c/c}$	Fusion 1	7 (33.3)	1 (4.8)	13 (61.9)	21
	Fusion 2	12 (32.4)	2 (5.4)	23 (62.2)	37
	Fusion 3	4 (50)	1 (12.5)	3 (37.5)	8
	Total	23 (38.6 ± 9.9)	4 (7.6 ± 4.3)	39 (53.9 ± 14.2)	66

RAG1$^{c/c}$ B lineage cells that have not yet completed D$_H$ to J$_H$ rearrangement on both alleles.

To determine the level of V$_H$DJ$_H$ versus DJ$_H$ rearrangements on the rearranged nonselected J$_H$ allele of RAG1$^{c/c}$ B lineage cells, we also quantified the number of DJ$_H$ and V$_H$-DJ$_H$ rearrangements in RAG1$^{c/c}$ and control B cell hybridomas. Southern blotting with a probe that hybridizes between the V$_H$ and D$_H$ gene segments demonstrated that 26 out of 42 (62%) and 12 out of 42 (28%) of the second alleles contained, respectively, DJ$_H$ and V$_H$DJ$_H$ rearrangements in control B cell hybridomas (Table I). In contrast, whereas the majority of RAG1$^{c/c}$ B cell hybridomas contained one allele in germline configuration, the remaining 23 out of 66 (35%) and 4 out of 66 (6%) of the nonproductive alleles contained, respectively, DJ$_H$ and V$_H$DJ$_H$ rearrangements (Fig. 5 and Table I). Therefore, there is a significant reduction in the percentage of RAG1$^{c/c}$ B cells containing V$_H$ to DJ$_H$ rearrangements on the nonproductive allele.

All RAG1$^{c/c}$ B cell hybridomas with germline J$_H$ loci also contained hybridizing sequences between the most J$_H$-proximal V$_H$ gene segment and the most 5′ D$_H$ gene segment (Fig. 5 C and Table I) (30), indicating lack of direct V$_H$ to D$_H$ rearrangements. In addition, we were unable to amplify direct V$_H$ to D$_H$ rearrangements in WT or RAG1$^{c/c}$ pro– or pre–B cell populations by PCR using sets of primers designed to amplify rearrangements involving the three V$_H$ gene segment families V$_H$558, V$_H$7183, and V$_H$Q52 and either DFL16 or DQ52 gene segments (unpublished data). Similarly, using an upstream V$_H$81X primer in conjunction with the D$_H$R primer that anneals to the 3′ RS sequence of DSP and DFL gene segment families (31), we were unable to amplify direct V$_H$81X to D$_H$ rearrangements (unpublished data). Thus, despite the notable reduction in D$_H$ to J$_H$ rearrangement, none of the RAG1$^{c/c}$ B lymphocytes appeared to have undergone direct V$_H$ to D$_H$ rearrangements on the nonselected second allele (Fig. 5 and Table I). Therefore, RAG1$^{c/c}$ mice exhibit a marked impairment in both D$_H$ to J$_H$ and V$_H$ to DJ$_H$ rearrangement.

RAG1$^{c/c}$ Mice Exhibit an Increased Level of D$_H$ to J$_H$ Inversional Hybrid Joints. We used a PCR strategy to compare the levels of normal and hybrid inversional D$_H$ to J$_H$ joints (DJ$_H$inv) between RAG1$^{c/c}$ and control mice (Fig. S3, available at http://www.jem.org/cgi/content/full/jem.20030627/DC1). Previous studies have shown that DJ$_H$inv joints occur in WT mice at levels ∼3 logs lower than normal D$_H$ to J$_H$ joints (47). Primary amplifications of DJ$_H$inv joints in DNA isolated from pro– and pre–B cells of both WT and RAG1$^{c/c}$ mice revealed an approximate three to fivefold increase in the levels of DJ$_H$inv joints detected in the latter (Fig. S3). To confirm that the amplified products observed were in fact the products of DJ$_H$inv rearrangements, we cloned and sequenced the junctions of 14 unique WT and 35 unique RAG1$^{c/c}$ DJ$_H$inv joints (Fig. S4, available at http://www.jem.org/cgi/content/full/jem.20030627/DC1). Consistent with previous studies (47), we estimate 13 of the 14 DJ$_H$inv joints cloned from WT mice and 31 out of 35 from RAG1$^{c/c}$ mice were hybrid joints (HJ), with the remainder likely being DJ$_H$inv coding joints (Fig. S4). These HJs form when the 23-bp RS previously associated with a J$_H$ gene segment becomes juxtaposed to a D$_H$–coding gene segment originally associated with a 12-bp RS, albeit in an inverted orientation (Fig. S3) (47). The junctions of HJs isolated from both WT and RAG1$^{c/c}$ mice frequently displayed a loss in D$_H$ coding sequence, and all but four of the RAG1$^{c/c}$ clones had P or N nucleotide additions (Fig. S4).

Discussion

Altered V(D)J Recombination in RAG1$^{c/c}$ Mice. We demonstrate that lymphocyte development and V(D)J recombination is modestly reduced in mice that express the core RAG1 protein in place of the WT RAG1 protein. The occurrence of significant levels of lymphocyte development in RAG1$^{c/c}$ mice is in accord with findings that the RAG1 core protein maintains substantial levels of cleavage activity in vitro. Thus, nearly 40% of the highly conserved RAG1 protein is not required to access RSSs and initiate V(D)J recombination in the context of chromosomal DNA. In addition, noncore regions of RAG-1 are not absolutely necessary for recruitment of factors required to complete the V(D)J recombination reaction in vivo. Moreover, the ab-

solute numbers of prolymphocytes are not as substantially reduced in RAG1$^{c/c}$ mice, as is found in NHEJ-deficient mice, suggesting that DNA DSBs initiated by the core RAG1 protein are properly repaired (48, 49). However, we cannot rule out a modest diminution in joining activities. Overall, RAG1$^{c/c}$ mice clearly exhibit an impairment in both B and T cell development at the pro to prelymphocyte transition, the same stage at which RAG1- (and RAG2-) deficient mice exhibit a complete developmental block (22, 23).

In normal mice, D to J rearrangements take place on both TCRβ or IgH alleles before V to DJ rearrangement (4–6). However, RAG1$^{c/c}$ mice develop mature lymphocytes with germline J_H loci on their nonproductive alleles, indicating that the noncore regions of RAG1 are required for fully efficient D to J rearrangement. Retention of germline J_H loci occurs despite the fact that D_H to J_H rearrangement initiates at an earlier developmental stage than V_H to DJ_H rearrangement (6). Expression of core RAG1 in the absence of WT protein also results in a reduced frequency of V_HDJ_H rearrangements on nonselected alleles that contain DJ_H rearrangements. Therefore, reduced frequency of both DJ_H and V_HDJ_H rearrangements on the nonselected alleles in RAG1$^{c/c}$ mice likely reflects a decrease in overall V(D)J recombination efficiency. The decreased levels of 3′ Dβ RS ends, which are associated with D to J rearrangements, along with the decreased levels of 5′ D_H and 5′ Dβ RS ends, which are associated with V to DJ rearrangements, further supports this conclusion. Of note, previous studies showed that Igκ and TCRα rearrangements were not reduced in RAG2$^{c/c}$ mice (20, 21) which was argued to reflect a correlation between recombination efficiency and specific RS sequence motifs (21). In this regard, we also find that $V_κ$ to $J_κ$ rearrangements are comparable between RAG1$^{c/c}$ and control mice and that the TCRα locus rearranges on both alleles of RAG1$^{c/c}$ T cells.

Although the above findings clearly demonstrate that overall V(D)J recombination is affected in RAG1$^{c/c}$ mice at the IgH and TCRβ loci, we cannot unequivocally rule out the possibility of more subtle effects of truncated core RAG1 on D to J versus V to DJ rearrangements. Notably, expression of core RAG1 in place of full-length RAG1 resulted in the same or even increased production of DJ_Hinv hybrid joints suggesting that noncore regions of RAG1 may preferentially favor this form of hybrid D to J join. In this regard, it is possible that the noncore region of RAG1 may contribute to the proper assembly or stability of synaptic and/or postcleavage complexes, thereby increasing overall recombination efficiency while leading to a decreased frequency of aberrant recombination products. This would be consistent with previous studies showing an increased frequency of hybrid joins and transposition events by core RAGs (17, 50, 51). However, we note that we cannot rule out the possibility that the steady-state increase in DJ_Hinv hybrid joins results from a decreased level of secondary DJ_H joins that would delete such rearrangements in normal preB cells.

V_H to DJ_H and Vβ to DJβ rearrangements were dramatically reduced in developing lymphocytes of mice that express core RAG2 in place of full-length RAG2 (20, 21). One study concluded that D to J recombination at the IgH and TCRβ loci was unaffected in core RAG2-expressing mice and showed that the reduction in V to DJ rearrangement correlated with decreased RAG cleavage activity at the 5′ D and V RSSs (21). A separate study found a similar effect on V to DJ rearrangements but clearly demonstrated through direct hybridoma analyses that D_H to J_H rearrangement was also impaired in core RAG2-expressing mice (20). However, V_HDJ_H rearrangements on nonselected alleles were not detected in core RAG2-expressing B cell hybridomas, suggesting that the homozygous core RAG2 mutation affects V_H to DJ_H rearrangement more substantially than D_H to J_H rearrangement (20, 21). In contrast, we have demonstrated V_HDJ_H rearrangements do occur on nonselected alleles of RAG1$^{c/c}$ B cell hybridomas and find that reduction in D to J and V to DJ rearrangements are accompanied by reduced cleavage at both 5′ and most 3′ D RSSs.

Implications of Altered V(D)J_H Rearrangement Patterns in RAG1$^{c/c}$ B Lineage Cells. Ordered assembly of IgH and TCRβ genes appears to be mediated through developmental stage-specific D versus V segment accessibility (4, 52). Our detection of mature B cells with nonrearranged IgH alleles demonstrates that the expression of core RAG1 in place of full-length RAG1 allows developing B cells to progress to a stage in which V_H to DJ_H rearrangement can take place in the absence of DJ_H rearrangements on both alleles. Thus, these studies indicate that there is no mechanistic requirement for D_H to J_H rearrangement on both alleles for progression to a developmental stage in which V_H gene segments become accessible. However, we did not detect direct V_H to D_H joins in the absence of DJ_H rearrangements in the RAG1$^{c/c}$ B cells. Although absence of direct V_H to D_H joins might be explained by recombinational efficiency, it would also be consistent with a mechanistic requirement for a D_H to J_H deletional rearrangement before a subsequent V_H to DJ_H rearrangement on the same allele. If so, V_H to DJ_H rearrangement may require deletion of sequences between D_HQ52 and the J_H1 gene segment and/or be specifically targeted only to an assembled DJ_H complex versus a nonrearranged upstream germline D_H segment. Thus, rearrangement may allow establishment of V_H gene accessibility, for example, by activating the 5′ D_H RSS via the germline D_H promoter, or may facilitate the capture or synapsis of V_H-associated RS target sequences. In the latter context, it is notable that deletion of the 3′ Dβ RSS allowed direct Vβ to Dβ joining in the absence of Dβ to Jβ joining (53), suggesting that the 3′ Dβ RSS may be responsible for maintaining ordered rearrangement, perhaps by providing a high affinity RAG binding site.

Putative Functions of Noncore RAG1 Regions. The NH_2 terminus of RAG1 contains a zinc finger ring domain involved in homodimerization (54) and cysteine-containing elements with suggested multimerization functions (19). The ring finger domain has E3 ubiquitin ligase activity, al-

though a physiological function has yet to be linked to this activity (55). In addition, three basic regions within the NH_2 terminus of RAG1 associate with SRP1 (56), a protein known to interact with nuclear localization sequences and to be involved in facilitating nuclear transport (57). Although mutations in these basic regions affect binding to SRP1, nuclear localization is not dramatically altered because there are additional nuclear localization sequences within the RAG1 core region (56). In this regard, we show that core RAG1 is expressed at somewhat higher levels than WT RAG1, with the majority of protein being located in the nucleus. Elevated expression of core RAG1 compared with full-length RAG1 probably reflects the deletion of sequences regulating its degradation (13, 16, 19).

The observation that both DJ_H and V_HDJ_H rearrangements are affected in RAG1$^{c/c}$ mice suggests the core RAG1 protein simply may be inefficient at mediating V(D)J recombination. Likewise, our PCR analyses indicate that the relative efficiencies of certain Vβ to DJβ rearrangements in RAG1$^{c/c}$ DP T cells is very similar to that of core RAG2-expressing T cells (21). In this context, the modest reduction in peripheral lymphocyte numbers probably reflects a selection and expansion of the few B and T cells that productively rearrange their antigen receptor genes. Although the nature of the V(D)J recombination defect is unclear, one could speculate that multimerization motifs within the noncore regions of RAG1 could be important for synapsis between cleavage complexes and/or other proteins associated with distant RS/coding gene segments, with early disassembly of the cleavage complex occurring in their absence. E3 ubiquitin ligases have been linked to protein degradation, cell cycle control, and DNA repair (58) and that such an activity is contained within the NH_2-terminal region of RAG1 raises some intriguing possibilities. For instance, it was shown recently that RAG2 is targeted for degradation by ubiquitination (59). Ubiquitination mediated by RAG1 could ensure that a RAG-associated complex is disassembled and removed from coding gene segments to allow for efficient ligation by NHEJ proteins. Another possibility would be that RAG1-dependent ubiquitination of histones flanking RAG-initiated DSBs may alter chromatin structure to facilitate subsequent repair (55, 60).

RAG Mutations and Immune Deficiencies. Mutations in both RAG1 and RAG2 can result in partial recombination activity that in humans can lead to T$^-$B$^-$ SCID and OS. One group of frameshift mutations identified in OS and OS-like patients leads to alternative ATG usage resulting in NH_2-terminally truncated RAG1 proteins (27, 28). In vitro experiments demonstrated that, like the core RAG1 protein, proteins encoded by these frameshift mutant alleles remain partially functional for V(D)J recombination; however, in vivo they lead to dramatically reduced lymphocyte numbers and to immune deficiency (27, 28). Although the NH_2-terminal truncation of the murine core RAG1 protein does not fully recapitulate the effects of the frameshift mutant alleles detected in these OS patients, RAG1$^{c/c}$ mice do exhibit some similar phenotypes. For example, germline

Dβ–Jβ sequences have been isolated from the T cells of OS patients, demonstrating incomplete TCRβ rearrangement (61). The targeted core RAG1 replacement results in the deletion of a larger stretch of NH_2-terminal sequences than the human frameshift mutations. Yet RAG1$^{c/c}$ mice have only slightly reduced numbers of B and T lymphocytes compared with OS patients that have variable T cell numbers but virtually undetectable B cells (26, 62). Many human RAG1 frameshift mutations result in decreased protein expression and cellular mislocalization (27), but core RAG1 in RAG1$^{+/c}$ mice is expressed at levels higher than that of full-length RAG1 protein and is expressed predominantly in the nucleus. Therefore, development of OS in patients with NH_2-terminal frameshift mutations may not simply be due to the absence of the noncore RAG1 regions but may also be influenced by reduction in the overall amount or localization of the truncated RAG1 protein. The generation of mice harboring mutations in RAG1 that directly mimic those found in human OS patients should provide insights into the relationship between RAG activity and the development of specific immune deficiencies.

References

1. Gellert, M. 2002. V(D)J recombination: rag proteins, repair factors, and regulation. *Annu. Rev. Biochem.* 71:101–132.
2. Bassing, C.H., W. Swat, and F.W. Alt. 2002. The mechanism and regulation of chromosomal V(D)J recombination. *Cell.* 109:S45–S55.
3. Hesslein, D.G., and D.G. Schatz. 2001. Factors and forces controlling V(D)J recombination. *Adv. Immunol.* 78:169–232.
4. Alt, F.W., G.D. Yancopoulos, T.K. Blackwell, C. Wood, E. Thomas, M. Boss, R. Coffman, N. Rosenberg, S. Tonegawa, and D. Baltimore. 1984. Ordered rearrangement of immunoglobulin heavy chain variable region segments. *EMBO J.* 3:1209–1219.
5. Born, W., J. Yague, E. Palmer, J. Kappler, and P. Marrack. 1985. Rearrangement of T-cell receptor beta-chain genes during T-cell development. *Proc. Natl. Acad. Sci. USA.* 82:2925–2929.
6. Hardy, R.R., C.E. Carmack, S.A. Shinton, J.D. Kemp, and K. Hayakawa. 1991. Resolution and characterization of pro-B and pre-pro-B cell stages in normal mouse bone marrow. *J. Exp. Med.* 173:1213–1225.
7. Kisielow, P., and H. von Boehmer. 1995. Development and selection of T cells: facts and puzzles. *Adv. Immunol.* 58:87–209.
8. Rolink, A.G., C. Schaniel, J. Andersson, and F. Melchers.

2001. Selection events operating at various stages in B cell development. *Curr. Opin. Immunol.* 13:202–207.

9. Fugmann, S.D., A.I. Lee, P.E. Shockett, I.J. Villey, and D.G. Schatz. 2000. The RAG proteins and V(D)J recombination: complexes, ends, and transposition. *Annu. Rev. Immunol.* 18:495–527.

10. Cuomo, C.A., and M.A. Oettinger. 1994. Analysis of regions of RAG-2 important for V(D)J recombination. *Nucleic Acids Res.* 22:1810–1814.

11. Sadofsky, M.J., J.E. Hesse, J.F. McBlane, and M. Gellert. 1993. Expression and V(D)J recombination activity of mutated RAG-1 proteins. *Nucleic Acids Res.* 21:5644–5650.

12. Sadofsky, M.J., J.E. Hesse, and M. Gellert. 1994. Definition of a core region of RAG-2 that is functional in V(D)J recombination. *Nucleic Acids Res.* 22:1805–1809.

13. Silver, D.P., E. Spanopolou, R.C. Mulligan, and D. Baltimore. 1993. Dispensable sequence motifs in the *RAG-1* and *RAG-2* genes for plasmid V(D)J recombination. *Proc. Natl. Acad. Sci. USA.* 90:6100–6104.

14. Kirch, S.A., P. Sudarsanam, and M.A. Oettinger. 1996. Regions of RAG1 protein critical for V(D)J recombination. *Eur. J. Immunol.* 26:886–891.

15. McMahan, C.J., M.J. Difilippantonio, N. Rao, E. Spanopoulou, and D.G. Schatz. 1997. A basic motif in the N-terminal region of RAG1 enhances V(D)J recombination activity. *Mol. Cell. Biol.* 17:4544–4552.

16. Steen, S.B., J. Han, C. Mundy, M.A. Oettinger, and D.B. Roth. 1999. Roles of the "dispensable" portions of RAG-1 and RAG-2 in V(D)J recombination. *Mol. Cell. Biol.* 19:3010–3017.

17. Sekiguchi, J.A., S. Whitlow, and F.W. Alt. 2001. Increased accumulation of hybrid V(D)J joins in cells expressing truncated versus full-length RAGs. *Mol. Cell.* 8:1383–1390.

18. Kirch, S.A., G.A. Rathbun, and M.A. Oettinger. 1998. Dual role of RAG2 in V(D)J recombination: catalysis and regulation of ordered Ig gene assembly. *EMBO J.* 17:4881–4886.

19. Roman, C.A., S.R. Cherry, and D. Baltimore. 1997. Complementation of V(D)J recombination deficiency in RAG-1(−/−) B cells reveals a requirement for novel elements in the N-terminus of RAG-1. *Immunity.* 7:13–24.

20. Akamatsu, Y., R. Monroe, D.D. Dudley, S.K. Elkin, F. Gartner, S.R. Talukder, Y. Takahama, F.W. Alt, C.H. Bassing, and M.A. Oettinger. 2003. Deletion of the RAG2 C terminus leads to impaired lymphoid development in mice. *Proc. Natl. Acad. Sci. USA.* 100:1209–1214.

21. Liang, H.E., L.Y. Hsu, D. Cado, L.G. Cowell, G. Kelsoe, and M.S. Schlissel. 2002. The "dispensable" portion of RAG2 is necessary for efficient V-to-DJ rearrangement during B and T cell development. *Immunity.* 17:639–651.

22. Shinkai, Y., G. Rathbun, K.-P. Lam, E.M. Oltz, V. Stewart, M. Mendelsohn, J. Charron, M. Datta, F. Young, A.M. Stall, and F.W. Alt. 1992. RAG-2-deficient mice lack mature lymphocytes owing to inability to initiate V(D)J rearrangement. *Cell.* 68:855–867.

23. Mombaerts, P., J. Iacomini, R.S. Johnson, K. Herrup, S. Tonegawa, and V.E. Papaioannou. 1992. RAG-1-deficient mice have no mature B and T lymphocytes. *Cell.* 68:869–877.

24. Santagata, S., A. Villa, C. Sobacchi, P. Cortes, and P. Vezzoni. 2000. The genetic and biochemical basis of Omenn Syndrome. *Immunol. Rev.* 178:64–74.

25. Schwarz, K., G.H. Gauss, L. Ludwig, U. Pannicke, Z. Li, D. Lindner, W. Friedrich, R.A. Seger, T.E. Hansen-Hagge, S. Desiderio, et al. 1996. RAG mutations in human B cell–negative SCID. *Science.* 274:97–99.

26. Villa, A., S. Santagata, F. Bozzi, S. Giliani, A. Frattini, L. Imberti, L.B. Gatta, H.D. Ochs, K. Schwarz, L.D. Notarangelo, et al. 1998. Partial V(D)J recombination activity leads to Omenn Syndrome. *Cell.* 93:885–896.

27. Santagata, S., C.A. Gomez, C. Sobacchi, F. Bozzi, M. Abinun, S. Pasic, P. Cortes, P. Vezzoni, and A. Villa. 2000. N-terminal RAG1 frameshift mutations in Omenn's Syndrome: internal methionine usage leads to partial V(D)J recombination activity and reveals a fundamental role in vivo for the N-terminal domains. *Proc. Natl. Acad. Sci. USA.* 97:14572–14577.

28. Noordzij, J.G., N.S. Verkaik, N.G. Hartwig, R. de Groot, D.C. van Gent, and J.J. van Dongen. 2000. N-terminal truncated human RAG1 proteins can direct T-cell receptor but not immunoglobulin gene rearrangements. *Blood.* 96:203–209.

29. Alt, F., N. Rosenberg, S. Lewis, E. Thomas, and D. Baltimore. 1981. Organization and reorganization of immunoglobulin genes in A–MuLV-transformed cells: rearrangement of heavy but not light chain genes. *Cell* 27:381–390.

30. Sakai, E., A. Bottaro, L. Davidson, B.P. Sleckman, and F.W. Alt. 1999. Recombination and transcription of the endogenous Ig heavy chain locus is effected by the Ig heavy chain intronic enhancer core region in the absence of the matrix attachment regions. *Proc. Natl. Acad. Sci. USA.* 96:1526–1531.

31. Schlissel, M.S., L.M. Corcoran, and D. Baltimore. 1991. Virally-transformed pre-B cells show ordered activation but not inactivation of immunoglobin gene rearrangement and transcription. *J. Exp. Med.* 173:711–720.

32. Gaertner, F., F.W. Alt, R. Monroe, M. Chu, B.P. Sleckman, L. Davidson, and W. Swat. 1999. Immature thymocytes employ distinct signaling pathways for allelic exclusion versus differentiation and expansion. *Immunity.* 10:537–546.

33. Roth, D.B., C. Zhu, and M. Gellert. 1993. Characterization of broken DNA molecules associated with V(D)J recombination. *Proc. Natl. Acad. Sci. USA.* 90:10788–10792.

34. van Gent, D.C., J.F. McBlane, D.A. Ramsden, M.J. Sadofsky, J.E. Hesse, and M. Gellert. 1996. Initiation of V(D)J recombination in a cell-free system by RAG1 and RAG2 proteins. *Curr. Top. Microbiol. Immunol.* 217:1–10.

35. Steen, S.B., L. Gomelsky, S.L. Speidel, and D.B. Roth. 1997. Initiation of V(D)J recombination in vivo: role of recombination signal sequences in formation of single and paired double-strand breaks. *EMBO J.* 16:2656–2664.

36. Mo, X., T. Bailin, and M.J. Sadofsky. 1999. RAG1 and RAG2 cooperate in specific binding to the recombination signal sequence in vitro. *J. Biol. Chem.* 274:7025–7031.

37. Gorman, J.R., N. van der Stoep, R. Monroe, M. Cogne, L. Davidson, and F.W. Alt. 1996. The Ig(kappa) enhancer influences the ratio of Ig(kappa) versus Ig(lambda) B lymphocytes. *Immunity.* 5:241–252.

38. Kuhn, R., K. Rajewsky, and W. Muller. 1991. Generation and analysis of interleukin-4 deficient mice. *Science.* 254:707–710.

39. von Boehmer, H., I. Aifantis, J. Feinberg, O. Lechner, C. Saint-Ruf, U. Walter, J. Buer, and O. Azogui. 1999. Pleiotropic changes controlled by the pre-T-cell receptor. *Curr. Opin. Immunol.* 11:135–142.

40. Sleckman, B.P., C.G. Bardon, R. Ferrini, L. Davidson, and F.W. Alt. 1997. Function of the TCR alpha enhancer in alphabeta and gammadelta T cells. *Immunity.* 7:505–515.

41. Mombaerts, P., A.R. Clarke, M.A. Rudnicki, J. Iacomini, S. Itohara, J.J. Lafaille, L. Wang, Y. Ichikawa, R. Jaenisch, M.L. Hooper, et al. 1992. Mutations in T-cell antigen receptor genes alpha and beta block thymocyte development at different stages. *Nature*. 360:225–231.

42. Casanova, J.L., P. Romero, C. Widmann, P. Kourilsky, and J.L. Maryanski. 1991. T cell receptor genes in a series of class I major histocompatibility complex-restricted cytotoxic T lymphocyte clones specific for a *Plasmodium berghei* nonapeptide: implications for T cell allelic exclusion and antigen-specific repertoire. *J. Exp. Med*. 174:1371–1383.

43. ten Boekel, E., F. Melchers, and A. Rolink. 1995. The status of Ig loci rearrangements in single cells from different stages of B cell development. *Int. Immunol*. 7:1013–1019.

44. Reth, M.G., S. Jackson, and F.W. Alt. 1986. V_HDJ_H formation and DJ_H replacement during pre-B differentiation: nonrandom usage of gene segments. *EMBO J*. 5:2131–2138.

45. Toda, M., T. Hirama, S. Takeshita, and H. Yamagishi. 1989. Excision products of immunoglobulin gene rearrangements. *Immunol. Lett*. 21:311–316.

46. Coffman, R.L., and I.L. Weissman. 1983. Immunoglobulin gene rearrangement during pre-B cell differentiation. *J. Mol. Cell. Immunol*. 1:31–41.

47. Sollbach, A.E., and G.E. Wu. 1995. Inversions produced during V(D)J rearrangement at IgH, the immunoglobulin heavy-chain locus. *Mol. Cell. Biol*. 15:671–681.

48. Gao, Y., J. Chaudhuri, C. Zhu, L. Davidson, D.T. Weaver, and F.W. Alt. 1998. A targeted DNA-PKcs-null mutation reveals DNA-PK-independent functions for KU in V(D)J recombination. *Immunity*. 9:367–376.

49. Gao, Y., Y. Sun, K.M. Frank, P. Dikkes, Y. Fujiwara, K.J. Seidl, J.M. Sekiguchi, G.A. Rathbun, W. Swat, J. Wang, et al. 1998. A critical role for DNA end-joining proteins in both lymphogenesis and neurogenesis. *Cell*. 95:891–902.

50. Elkin, S.K., A.G. Matthews, and M.A. Oettinger. 2003. The C-terminal portion of RAG2 protects against transposition in vitro. *EMBO J*. 22:1931–1938.

51. Tsai, C.L., and D.G. Schatz. 2003. Regulation of RAG1/RAG2-mediated transposition by GTP and the C-terminal region of RAG2. *EMBO J*. 22:1922–1930.

52. Tourigny, M.R., S. Mazel, D.B. Burtrum, and H.T. Petrie. 1997. T cell receptor (TCR)-beta gene recombination: dissociation from cell cycle regulation and developmental progression during T cell ontogeny. *J. Exp. Med*. 185:1549–1556.

53. Sleckman, B.P., C.H. Bassing, M.M. Hughes, A. Okada, M. D'Auteuil, T.D. Wehrly, B.B. Woodman, L. Davidson, J. Chen, and F.W. Alt. 2000. Mechanisms that direct ordered assembly of T cell receptor beta locus V, D, and J gene segments. *Proc. Natl. Acad. Sci. USA*. 97:7975–7980.

54. Rodgers, K.K., I.J. Villey, L. Ptaszek, E. Corbett, D.G. Schatz, and J.E. Coleman. 1999. A dimer of the lymphoid protein RAG1 recognizes the recombination signal sequence and the complex stably incorporates the high mobility group protein HMG2. *Nucleic Acids Res*. 27:2938–2946.

55. Yurchenko, V., Z. Xue, and M. Sadofsky. 2003. The RAG1 N-terminal domain is an E3 ubiquitin ligase. *Genes Dev*. 17:581–585.

56. Spanopoulou, E., P. Cortes, C. Shih, C.M. Huang, D.P. Silver, P. Svec, and D. Baltimore. 1995. Localization, interaction, and RNA binding properties of the V(D)J recombination-activating proteins RAG1 and RAG2. *Immunity*. 3:715–726.

57. Weis, K., I.W. Mattaj, and A.I. Lamond. 1995. Identification of hSRP1 alpha as a functional receptor for nuclear localization sequences. *Science*. 268:1049–1053.

58. Weissman, A.M. 2001. Themes and variations on ubiquitylation. *Nat. Rev. Mol. Cell Biol*. 2:169–178.

59. Mizuta, R., M. Mizuta, S. Araki, and D. Kitamura. 2002. RAG2 is down-regulated by cytoplasmic sequestration and ubiquitin-dependent degradation. *J. Biol. Chem*. 277:41423–41427.

60. Jason, L.J., S.C. Moore, J.D. Lewis, G. Lindsey, and J. Ausio. 2002. Histone ubiquitination: a tagging tail unfolds? *Bioessays*. 24:166–174.

61. Brooks, E.G., A.H. Filipovich, J.W. Padgett, R. Mamlock, and R.M. Goldblum. 1999. T-cell receptor analysis in Omenn's Syndrome: evidence for defects in gene rearrangement and assembly. *Blood*. 93:242–250.

62. Corneo, B., D. Moshous, T. Gungor, N. Wulffraat, P. Philippet, F.L. Le Deist, A. Fischer, and J.P. de Villartay. 2001. Identical mutations in RAG1 or RAG2 genes leading to defective V(D)J recombinase activity can cause either T-B-severe combined immune deficiency or Omenn syndrome. *Blood*. 97:2772–2776.

63. Schlissel, M., A. Constantinescu, T. Morrow, M. Baxter, and A. Peng. 1993. Double-strand signal sequence breaks in V(D)J recombination are blunt, 5′ phosphorylated, RAG-dependent, and cell-cycle-regulated. *Genes Dev*. 7:2520–2532.